

Expression Pattern of Ngf in Astrocytes after Spinal Cord Injury and the Clinical Significance

Zengqiang Liu, Bo Song*

Department of Neurosurgery, Xianyang Hospital of Yan'an University, Xianyang, Shaanxi, 712000, China

ARTICLE INFO

Original paper

Article history:

Received: August 10, 2021

Accepted: November 29, 2021

Published: December 30, 2021

Keywords:

Spinal cord injury; oxidative stress; astrocytes; neuroglobin

ABSTRACT

In the current study, we evaluated the expression pattern of neuroglobin (Ngf) in the astrocytes after spinal cord injury (SCI) and explore the clinical significance. For this purpose, a total of 48 Sprague-Dawley rats were divided into the SCI group (n = 40) and Sham group (n = 8). Rats in the SCI group were used to prepare the SCI models by using the modified Allen's method, followed by the HE staining to observe the post-SCI pathological changes and immunofluorescent staining to observe the dynamic changes of Ngf in astrocytes after SCI. Then, oxidative stress injury models were constructed on the astrocytes in the spinal cord of rats by using peroxide in different concentrations (0, 50, 100, 150, 200 and 400 μ mol/L), and at 6 and 12 h after treatment, the vitality of astrocytes that were treated by peroxide in different concentrations was determined using the MTT method, while the ability of astrocytes to generate radical oxygen species (ROS) was determined by using the flow cytometry. The mRNA expression of Ngf after the oxidative stress injury in astrocytes was measured by using the real-time quantitative PCR. Results of HE staining demonstrated that rats with SCI presented with the gradual transition from acute injury into the glial scar, a natural repair, while the results of immunofluorescent staining indicated that after SCI, expression of Ngf in the astrocytes experienced an increase followed by a decrease, and the peak level was attained at 14 d after SCI. Following the treatment of H₂O₂ at different concentrations (50, 100, 150, 200 and 400 μ mol/L) for 6 and 12 h, the vitality of astrocytes in the model groups was significantly lower than that in the control groups (all P < 0.05). As the concentration of H₂O₂ increased (50, 100, 150, 200, 400 μ mol/L) and exposure to H₂O₂ prolonged (6, 12 h), mRNA expression was firstly increased but then decreased in astrocytes in a time-dose dependent pattern (all P < 0.05). After SCI, the expression of Ngf in the astrocytes of spine was upregulated, suggesting that Ngf may be involved in the anti-oxidative stress injury in astrocytes after SCI, thereby playing as an endogenous protector of cells.

DOI: <http://dx.doi.org/10.14715/cmb/2021.67.6.22>

Copyright: © 2021 by the C.M.B. Association. All rights reserved.



Introduction

Spinal cord injury (SCI) is divided into the primary and secondary types, where primary SCI presents mainly with the neuronal necrosis, rupture of nerve fibers, damaged blood-spinal cord barrier and vascular injury (1), while the secondary SCI preliminarily with the cell apoptosis and progressive axonal loss, mainly including the ischemia and hypoxia in microcirculation, oxidative stress injury, excitatory amino acid poisoning and inflammatory responses (2). Research has shown that oxidative stress injury is critical to the development and progression of secondary SCI (3). Accumulated radical oxygen specimens (ROS) can cause oxidative stress injury to the spinal cord tissue, mainly involving the lipid peroxidation of the membrane, damage to the nucleic

acid and proteins, inhibition of enzyme system in oxidation respiratory chain, nerve fiber degeneration and delineation, eventually exacerbating the dysfunction and damage of spinal cord functions (4-7). Astrocytes are a group of cells that are mostly distributed and richest in the central nerve system, and they, as reported, could protect neurons by secreting the neurotrophic factors, alleviating the oxidative stress injury and pre-adapting to the ischemia (8). Following SCI, the formation of an astrocytic scar could mitigate the nervous inflammatory responses and inhibit the delineation of axons and nerve fibers to protect the neurons from secondary injury (9). Anderson et al. reported that astrocytic scar is conducive to post-SCI axonal regeneration (10). It has been reported that the post-SCI activation of

*Corresponding author. E-mail: 2298793130@qq.com
Cellular and Molecular Biology, 2021, 67(6): 160-166

astrocytes is a potential target for protecting the spinal cord function and repair (11, 12). Ngb is an oxygen-carrying globin in the cytoplasm that is mainly distributed in the nerve system, retinal cells and endocrine tissues (13). In brain injury, cerebral malaria and autoimmune encephalitis, Ngb is not only expressed in neurons but also in the reactive astrocytes in the injured regions and is associated with the formation of astrocytic scar (14, 15). The post-SCI protective effect of Ngb on the neurons has been frequently reported in the current literatures, but the role of Ngb in astrocytes has not yet been reported. From January 2020 to February 2021, we explored the changes in the expression pattern of Ngb in the astrocytes in SCI animal models and the role of Ngb in protecting the astrocytes from the oxidative stress injury in the cell models.

Materials and methods

Materials

A total of 48 female SD rats (3 months old, weight between 250 and 300 g) and 16 neonatal SD rats were provided by the Laboratory Animal Center of Xianyang Hospital. Major reagents: H₂O₂ (Sigma, USA); rabbit anti-rat GFAP and mouse anti-rat anti-Ngb antibody (Abcam, UK), donkey anti-rabbit Cy3 and donkey anti-mouse FITC (Antgene, Wuhan, China); fetal bovine serum (FBS) (BI, Israel); DMEM high-glucose medium (Thermo, USA), TRIzol reagent (MRC, USA), PCR primers (Sangon, Shanghai, China); reverse transcription kit (Fermentas, USA). Major apparatuses: IX71 fluorescent microscope (Olympus, Japan), CO₂ incubator (Thermo, USA), FACS flow cytometer (BD, USA), Multiscan Microplate Reader (Biotek, USA), real-time quantitative PCR apparatus (Rotor-Gene, Australia).

Preparation of SCI models

The 48 SD rats were divided into two groups randomly – the Sham group (n = 8) and the SCI group (n = 40). Modified Allen's method was used to prepare the SCI models on rats (16). In brief, rats, after being anesthetized by 10% chloral hydrate (350 mg/kg), were fixed on the operating table to remove the hair. With the junction between the floating rib and the 13th thoracic vertebra as a mark, an incision in the length of 3 cm was made along the linea mediana posterior to expose the paravertebral soft

tissues, and the T10 spinal cord was exposed by removing the spinal processes and vertebral plate. A 10 g bar was used to hit the T10 spinal dura mater by falling freely from the height at 25 mm, and 10 s later, the moderate injury was made to the spinal cord. The incision was then sutured, while rats were fed in the separated cages. Criteria for the successful construction of SCI model: bleeding of the spinal cord, distended spinal dura mater in amaranth, the tail of rats in spasmodic movement, low limbs and soma of rats in retracting movement, rats in delayed paralysis. This study had been approved by the Ethical Committee for Laboratory Animals of Yan'an University.

Sample collection of the spinal cord and HE staining

At 1, 3, 7, 14 and 28 days after surgery, 8 rats and 5 rats were selected randomly from the SCI group and the sham group, respectively. Following anesthesia, the heart of the rat was exposed, and normal saline in the volume of 250 mL was perfused through the intubation via the ascending aorta. Perfusion was terminated when colorless, clear fluid effused from the auricula dextra, and paraformaldehyde was then perfused. Subsequently, the injured spinal cord was taken out from the vertebrae and fixed in 4% paraformaldehyde for paraffin-embedding and slicing into the sections in thickness of 4 μm for HE staining. At 1 h after SCI, the spinal cord was taken out, presenting with continuous interruption, severe degeneration and necrosis on the surface and surrounding the injured site, while rats in the sham group showed the integrated spinal cord, with no evident bleeding or necrosis.

Collection and identification of the spinal astrocytes

The neonatal Sprague-Dawley rats aged 1 or 2 days were immersed in 75% ethanol and then sacrificed to obtain the spinal cord on a super clean bench, where the spinal cord and vessels were dissected and cut into pieces in the cold PBS. After being digested in 0.25% trypsin at room temperature for 15 min, tissue samples were placed into the 12% FBS-DMEM to prepare the cell suspension. The cell suspension was then filtrated by using the 200-mesh filter, centrifuged, resuspended and seeded onto the T25 culture flask, where the

fibroblasts were removed by the method of differential adhesion, and the medium was refreshed at 24 h initially, then every 2 to 3 days. After being cultured for 6 – 8 days, cells in 90% of confluence were shaken horizontally at 160 r/min and 37°C for 16–18 h to remove the oligodendrocytes and microglial cells. When cells were subcultured to the third generation (about 21 days), a few cells were selected for identification of astrocytes and purity via the GFAP- and DAPI-labeled fluorescent staining. Within the stained vision, we could see the closely arranged protrusions of the GFAP-positive cells, and GFAP- and DAPI-positive cells took up more than 90% of the total cells. Thus, astrocytes in the third generation were selected for the following experiments.

GFAP and Ngb immunofluorescent staining

Astrocytes in the 3rd generation were seeded into the gelatin-coated 24-well plate at a density of 1×10^5 /mL, and at a confluence of 80% or so, cells were rinsed three times in the cold PBS and then fixed in 4% paraformaldehyde for 30 min at 4°C, followed by 3 washes in PBS. Following procedures were performed as the method mentioned above to observe the expression of GFAP and Ngb in the astrocytes.

Detection of astrocyte viability

In this part, an MTT assay was performed. In brief, astrocytes in the 3rd generation were seeded on a 96-well plate at a density of 5×10^4 /mL, with 200 μ L in each well, and cultured in a CO₂ thermostat incubator for 72 h. At a confluence of 80% or so, cells were treated by H₂O₂ at different concentrations (0, 50, 100, 150, 200 and 400 μ mol/L) for different times (6 or 12 h) for later MTT assay. The absorbance of each well at a wavelength of 490 nm was also determined using the full-wave microplate reader, and cell viability were calculated by using the following formula: Cell viability = (A treatment group – A reference) / (A control group – A reference) \times 100%.

Generation of endogenous ROS in astrocytes

Flow cytometry was adopted in this part. AS in the third generation was seeded in a 6-well plate at a density of 1.25×10^5 /mL, with 2 mL in each well. Following 72 hours of culture, cells were treated with H₂O₂ in varying concentrations (50, 100, 200 and 400

μ mol/L) for different times (6 and 12 h) and then digested in trypsin. Thereafter, cells were resuspended to prepare the cell suspension, where a DCFH-DA probe was added and the final concentration was adjusted to 10 μ mol/L. After 1 hour of incubation at 37°C, cells were rinsed in the serum-free medium and centrifuged. Cells in the sediment were resuspended in 2% FBS-DMEM and subjected to the measurement in a flow cytometer.

Detection of mRNA expression of Ngb, SOD₂ and CAT

Real-time quantitative PCR was adopted in this study. AS, after being treated by H₂O₂ in varying concentrations (50, 100, 200 and 400 μ mol/L) for different times (6 and 12 h), were subjected to the extraction of total mRNA by using the TRIzol reagent. With 1 μ g total RNA, cDNA was prepared by using the reverse transcription kit and then diluted to the concentration of 5 ng/ μ L, followed by the fluorescent quantitative PCR with SYBR Green PCR Master Mix and corresponding primers: Ngb, forward primer 5'-GGCCATCCAAGAGAGGTGAT-3' and reverse primer 5'-CCATGCCTCCTCACTACCAA-3'; SOD₂, forward primer 5'-CTGCTGGGGATTGATGTGTG-3' and reverse primer 5'-CTACAAAACACCCACCACGGCAT-3'; CAT, forward primer 5'-GCGGATTCCTGAGAGAGTGG-3' and reverse primer 5'-GAATCGGACGGCAATAGGAG-3'. The reaction system was set as follow: 95°C for 2 min, 95°C for 5 s, 60°C for 30 s, 72°C for the 30s, 72°C for 5 min, a total of 35 cycles. Relative expression of the targeted gene was calculated by the method of $2^{-\Delta\Delta Ct}$.

Statistical analysis

SPSS 20.0 software was used to perform the statistical analysis. Measurement data were expressed by mean \pm standard deviation (SD), and the data in normal distribution were compared by using the one-way analysis of variance, followed by LSD-t test for pairwise comparison. Comparison between two groups was performed by using t-test for independent samples. $P < 0.05$ suggested that the difference had statistical significance.

Results and discussion

Expression of GFAP and Ngf in AS after SCI

In the sham group, Ngf was low expressed in the spine, while GFAP-positive cells were distributed sporadically; in the white matter, AS were small, with thin and straight protrusions but fewer branches. On the margin of the white matter, a few cells were co-expressing GFAP and Ngf in the cytoplasm, with weak signals. At 1 d after the operation, the spinal structure was destroyed massively, and surrounding the injured site, the quantity of Ngf-positive cells increased. As compared to the sham group, co-expression of GFAP and Ngf was upregulated slightly. At 3 d after the operation, Ngf was upregulated continuously and co-expression of GFAP and Ngf surrounding the injured site also increased evidently. Upregulation of GFAP was observed 1 week after the operation, mainly at the margin of the surrounding site. Similarly, co-expression of GFAP and Ngf also increased, significantly higher than the region closing to the non-injured site. At the 14th and 28th days after the operation, the most evident increase in the expression of GFAP was seen, and the peak level was attained at the 28th day, with a significant augment in the number of protrusion of AS cells forming the compact network and the boundary between the lumen and cavity, while in the surrounding region, the peak level of co-expression of GFAP and Ngf was observed at the 14th day and began to decline from the 28th day.

Changes in the viability of AS cells under the treatment of H₂O₂ in varying concentrations and different time

After treatment of H₂O₂ for 6 h or 12 h, with the increase in the concentration of H₂O₂, viability of AS decreased gradually (F_{6h} =137.36, P < 0.01; F_{12h}=143.61, P < 0.001). Following 6 hours of treatment of H₂O₂, no significant difference was shown in the comparison of the viability of AS treated by H₂O₂ in the concentration of 100 μmol/L and 150 μmol/L (P = 0.158). Likewise, we found no significant difference in comparison of the viability of AS treated by H₂O₂ in the concentration of 150 μmol/L and 200 μmol/L at 12 h (P = 0.168). Thus, 50, 100, 200 and 400 μmol/L were determined as the concentrations of H₂O₂ in the following experiments. As the time of treatment extended, the viability of AS treated by

H₂O₂ in the same concentration decreased continuously, while no significant difference was shown in the comparison of the viability of AS treated by H₂O₂ in the concentration of 50 μmol/L (Table 1).

Table 1. Changes in the viability of AS treated by H₂O₂ in different concentrations or for different times (% , mean ± SD)

Time	AS viability					
	0 μmol/L	50 μmol/L	100 μmol/L	150 μmol/L	200 μmol/L	400 μmol/L
6 h	99.5±0.2	86.4±9.2*	76.7±2.6*	71.9±12.3*	60.4±4.2*	19.3±2.9*
12 h	98.9±0.9	77.2±13.8#	61.8±2.8#	51.1±4.4#	46.1±9.2#	10.4±1.4#
t	1.84	1.57	10.82	4.47	3.97	7.75
P	0.092	0.137	0.000	0.002	0.001	0.000

Note: * P < 0.01 vs. the cells that were not exposed to H₂O₂ at 6 h; # P < 0.001 vs. the cells that were not exposed to H₂O₂ at 12 h.

Generation of ROS induced by H₂O₂ for 6 and 12 h

H₂O₂ could induce the generation of ROS in AS. Within 6 h, ROS generation increased gradually as the H₂O₂ concentration increased, with the right-skewed peak level (F = 262.33, P < 0.01). Following exposure to H₂O₂ for 12 h, ROS generation in AS increased firstly and then decreased (F = 297.30, P < 0.01), and the peak level was attained in AS treated by H₂O₂ in the concentration of 100 μmol/L (Figure 1 and 2).

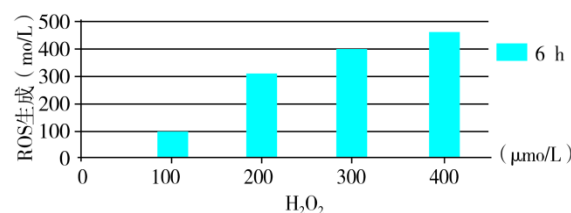


Figure 1. ROS generation in AS induced by H₂O₂ for 6 h

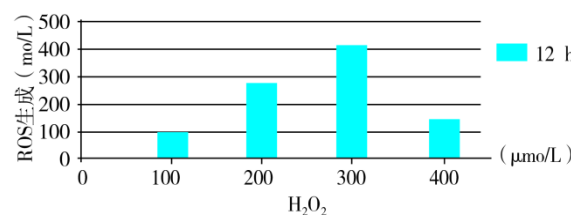


Figure 2. ROS generation in AS induced by H₂O₂ for 12 h

Changes in the mRNA expression of Ngf, SOD₂ and CAT under the induction of H₂O₂ at different time points

Following exposure to H₂O₂ at concentration between 50 and 400 μmol/L for 6 or 12 h, mRNA expression of Ngf increased firstly but then decreased (F_{6h}=67.48, P < 0.01; F_{12h}=51.47, P < 0.01), and the peak level was attained at 6 or 12 h in concentration

of 100 $\mu\text{mol/L}$ ($t = 4.72$; $P = 0.042$). Similarly, mRNA expression of CAT and SOD₂ also increased firstly but then decreased (CAT:F6h=95.31, $P < 0.001$;F12h = 101.20, $P < 0.001$, SOD₂ :F6h=94.73, $P < 0.001$;F 12h=41.54, $P < 0.01$), while after exposure to H₂O₂ at concentration of 100 $\mu\text{mol/L}$ for 12 h, the expression of SOD₂ was higher than the exposure for 6 h ($t = 6.78$, $P = 0.032$). The peak level of mRNA expression of Ngf, CAT and SOD₂ was attained in concentration of 50 $\mu\text{mol/L}$ or 100 $\mu\text{mol/L}$, followed by continuous decreases, the lowest level was shown in concentration of 400 $\mu\text{mol/L}$, and such changes were in a dose-time-dependent manner (all $P < 0.05$; Figure 3A, B and C).

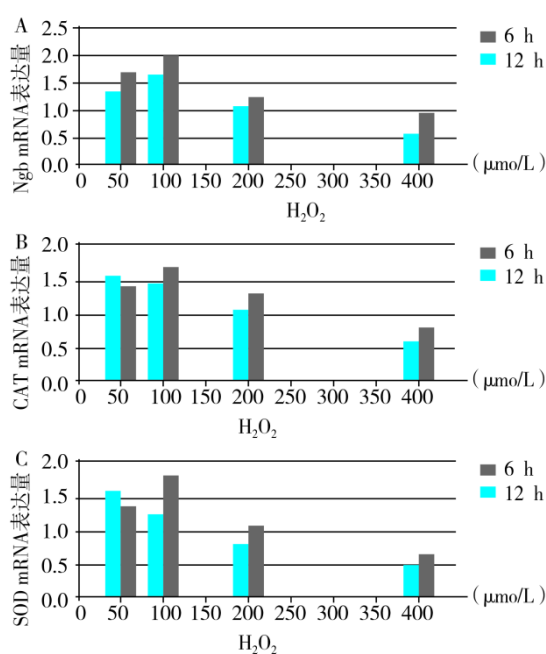


Figure 3. Expression of anti-oxidative stress genes in AS after exposure to H₂O₂

Oxidative stress injury refers to an imbalanced status of pro-oxidant and antioxidant, resulting in the excessive generation of free radicals, the tendency to oxidation, infiltration of neutrophils, increases in the protease secretion and massive generation of oxidative intermediate (17). Bermudez *et al.* (18) reported that oxidative stress exists continuously in the acute or chronic phase of SCI. Amri *et al.* (19) also found that H₂O₂ in the concentration of 100 $\mu\text{mol/L}$ can trigger the atrophy of AS and collapse in the glial network, with a decrease in cell density, while the treatment of Ngf could reverse changes above and exert the anti-apoptotic effect via reducing the generation of ROS

and downregulating the expression of pro-inflammatory factors (19).

CNS in mammals lacks the regeneration ability, and in rodent animals, the spinal function could be restored naturally to some extent after the acute phase of SCI besides the complete transection spinal cord injury (20). For cell response to the CNS injury, human beings evolve seemingly to isolate the minor injury and prevent the infection in the injured site, instead of repairing the large or irreparable injury, which coincides with the behaviors of AS (21, 22). After SCI, neurons, as compared to the AS, are more susceptible to the attack of ROS, while AS could protect the neurons from the oxidative stress injury, which may correlate with the abundant content of antioxidants (like glutathione and vitamin E) and the natural selection in cell evolution (23).

Current research has shown that SCI could trigger the proliferation and activation of AS, and the activated AS can further inhibit the expansion of the SCI region, eliminate the cell debris and remodel the injured site (24). Nathan *et al.* (25) reported that the spinal environment is the key that alters the fortune of AS. Okada *et al.* (9) confirmed that during the recovery from SCI, the knockout of gene inhibiting the activation of Socs3 in AS could enhance the abilities of AS in migration, isolating the injured site and restricting the dissemination of inflammation. In this study, we confirmed that in the natural recovery from SCI, SCI could enhance the expression of Ngf in AS. In the early stage of SCI, the upregulation of Ngf may associate with the increase in the oxygen supply to the injured site. Ever since the 7th day after SCI, co-expression of GFAP and Ngf is upregulated, and the peak level is attained at the 14th day when the formation rate of glial scar is also the fastest, which coincides with the function of AS. Thus, Ngf may facilitate the activation of AS, thereby promoting the natural recovery of SCI. However, during the 1st day to the 28th day after SCI, Ngf expression presents with an increase and then a decrease, suggesting that in addition to the activation of AS, Ngf also plays a role in anti-oxidation and -stress injury, which coincides with the findings of Amri *et al.* (19) and Fabrizio *et al.* (26).

ROS is an indicator reflecting the level of oxidative stress. Results of this study indicate that after 6 or 12 h of treatment by H₂O₂ in varying concentrations,

spinal cells presented with the oxidative stress injury in varying degrees, with significant declines in the viability of AS in a dose-dependent manner. Results of real-time PCR showed that H₂O₂-induced oxidative stress injury in AS could upregulate the expression of SOD₂, CAT and Ngb, and with the increase in the concentration of H₂O₂ and prolongation of exposure, the mRNA levels of SOD₂ and CAT, the endogenous anti-oxidative stress enzymes, also had an increase and then a decrease. Moreover, the mRNA expression of Ngb also showed expression patterns similar to the expression of SOD₂ and CAT, and the peak level was attained at a concentration of 100 µmol/L suggests that Ngb has a similar effect and is involved in the anti-oxidative stress injury together with SOD₂ and CAT. Douiri *et al.* (27) treated the H₂O₂-injured AS with the exogenous Ngb and found that Ngb could upregulate the mRNA expression of SOD₂ and CAT evidently, thereby antagonizing the oxidative stress injury, while inhibiting the activity of endogenous antioxidant system in AS could curb the protective effect of endogenous molecules on cell survival.

The results of this study confirmed that SCI could upregulate the expression of Ngb in AS and that Ngb may be involved in the antioxidative stress injury to AS after SCI, thereby advancing the natural recovery of cells from SCI. These findings lay the theoretical foundation for the involvement of astrocytes and neuroglobin in the treatment of SCI.

Acknowledgements

None.

Interest conflict

None.

References

- Colón JM, Miranda JD. Tamoxifen: an FDA approved drug with neuroprotective effects for spinal cord injury recovery. *Neural Regen Res* 2016; 11(8): 1208.
- Siddiqui AM, Khazaei M, Fehlings MG. Translating mechanisms of neuroprotection, regeneration, and repair to treatment of spinal cord injury. *Prog Brain Res* 2015; 218: 15-54.
- Fatima G, Sharma V, Das S, Mahdi A. Oxidative stress and antioxidative parameters in patients with spinal cord injury: implications in the pathogenesis of disease. *Spin Cord* 2015; 53(1): 3-6.
- Kazemi E, Zargooshi J, Dehpahni MF et al. Androgen regulated protein and pyruvate dehydrogenase kinase 4 in severe erectile dysfunction: A gene expression analysis, and computational study of protein structure. *Cell Mol Biol* 2021; 67(2): 89-94.
- Bilal I, Xie S, Elburki MS, Azizaram Z, Ahmed SM, Jalal ST. Cytotoxic effect of diferuloylmethane, a derivative of turmeric on different human glioblastoma cell lines. *Cell Mol Biomed Rep* 2021; 1(1): 14-22.
- Yu Z, Poppe JL, Wang X. Mitochondrial mechanisms of neuroglobin's neuroprotection. *Oxid Med Cell Longev* 2013; 2013.
- Stepien KM, Heaton R, Rankin S et al. Evidence of oxidative stress and secondary mitochondrial dysfunction in metabolic and non-metabolic disorders. *J Clin Med* 2017; 6(7): 71.
- Guo G, Bhat NR. Hypoxia/reoxygenation differentially modulates NF-κB activation and iNOS expression in astrocytes and microglia. *Antioxid Redox Signal* 2006; 8(5-6): 911-918.
- Okada S, Nakamura M, Katoh H et al. Conditional ablation of Stat3 or Socs3 discloses a dual role for reactive astrocytes after spinal cord injury. *Nature Med* 2006; 12(7): 829-834.
- Anderson MA, Burda JE, Ren Y et al. Astrocyte scar formation aids central nervous system axon regeneration. *Nature* 2016; 532(7598): 195-200.
- Shadhin KA, Hasan MR, Paul BK et al. Analysis of topological properties and drug discovery for bipolar disorder and associated diseases: A bioinformatics approach. *Cell Mol Biol* 2020; 66(7): 152-160.
- Watson JL, Hala TJ, Putatunda R, Sannie D, Lepore AC. Persistent at-level thermal hyperalgesia and tactile allodynia accompany chronic neuronal and astrocyte activation in superficial dorsal horn following mouse cervical contusion spinal cord injury. *PLoS One* 2014; 9(9): e109099.
- Brittain T. The anti-apoptotic role of neuroglobin. *Cells* 2012; 1(4): 1133-1155.
- Baez E, Echeverria V, Cabezas R, Ávila-Rodríguez M, Garcia-Segura LM, Barreto GE. Protection by neuroglobin expression in brain

- pathologies. *Front Neurol* 2016; 7: 146.
15. DellaValle B, Hempel C, Kurtzhals JA, Penkowa M. In vivo expression of neuroglobin in reactive astrocytes during neuropathology in murine models of traumatic brain injury, cerebral malaria, and autoimmune encephalitis. *Glia* 2010; 58(10): 1220-1227.
 16. Li J, Guo W, Xiong M et al. Erythropoietin facilitates the recruitment of bone marrow mesenchymal stem cells to sites of spinal cord injury. *Exp Ther Med* 2017; 13(5): 1806-1812.
 17. Darvishi E, Azizaram Z, Yari K et al. Lack of association between the TNF- α -1031 genotypes and generalized aggressive periodontitis disease. *Cell Mol Biol* 2016; 62(11): 63-66.
 18. Bermudez S, Khayrullina G, Zhao Y, Byrnes KR. NADPH oxidase isoform expression is temporally regulated and may contribute to microglial/macrophage polarization after spinal cord injury. *Mol Cell Neurosci* 2016; 77: 53-64.
 19. Amri F, Ghouili I, Amri M, Carrier A, Masmoudi-Kouki O. Neuroglobin protects astroglial cells from hydrogen peroxide-induced oxidative stress and apoptotic cell death. *J Neurochem* 2017; 140(1): 151-169.
 20. Hilton BJ, Bradke F. Can injured adult CNS axons regenerate by recapitulating development? *Development* 2017; 144(19): 3417-3429.
 21. Zambusi A, Ninkovic J. Regeneration of the central nervous system-principles from brain regeneration in adult zebrafish. *World J Stem Cell* 2020; 12(1): 8.
 22. Ercisli MF, Lechun G, Azeez SH, Hamasalih RM, Song S, Azizaram Z. Relevance of genetic polymorphisms of the human cytochrome P450 3A4 in rivaroxaban-treated patients. *Cell Mol Biomed Rep* 2021; 1(1): 33-41.
 23. Sekine Y, Lin-Moore A, Chenette DM et al. Functional genome-wide screen identifies pathways restricting central nervous system axonal regeneration. *Cell Rep* 2018; 23(2): 415-428.
 24. Arbo BD, Benetti F, Ribeiro MF. Astrocytes as a target for neuroprotection: modulation by progesterone and dehydroepiandrosterone. *Prog Neurobiol* 2016; 144: 27-47.
 25. Nathan FM, Li S. Environmental cues determine the fate of astrocytes after spinal cord injury. *Neural Regen Res* 2017; 12(12): 1964.
 26. Fabrizio A, Andre D, Laufs T et al. Critical re-evaluation of neuroglobin expression reveals conserved patterns among mammals. *Neuroscience* 2016; 337: 339-354.
 27. Douiri S, Bahdoudi S, Hamdi Y et al. Involvement of endogenous antioxidant systems in the protective activity of pituitary adenylate cyclase-activating polypeptide against hydrogen peroxide-induced oxidative damages in cultured rat astrocytes. *J Neurochem* 2016; 137(6): 913-930.